Polarization anisotropy of transient carrier and phonon dynamics in carbon nanotubes

Ji-Hee Kim,[1] Jaegyu Park,[1] Bong Yeon Lee,[1] Donghan Lee,[1] Ki-Ju Yee,[1,a)] Yong-Sik Lim,[2] Layla G. Booshehri,[3] Erik H. Hároz,[3] Junichiro Kono,[3] and Sung-Hoon Baik[4]
[1]*Department of Physics, Chungnam National University, Daejeon 305-764, Republic of Korea*
[2]*Department of Applied Physics, Konkuk University, Chungbuk 380-701, Republic of Korea*
[3]*Department of Electrical and Computer Engineering, Rice University, Houston, Texas 77005, USA*
[4]*Quantum Optics Research Division, Korea Atomic Energy Research Institute, Daejeon 305-353, Republic of Korea*

(Received 5 January 2009; accepted 3 April 2009; published online 20 May 2009)

We report on polarization-dependent transient carrier dynamics and coherent phonon oscillations in single-walled carbon nanotubes by determining the relation between the nanotube axis and the incident light polarization. Due to the anisotropic shape of nanotubes, optical absorption strongly depends on the polarization direction. We observed three decay components when the excitation wavelength was resonant with the E_{22} transition energy and observed two-decay components under off-resonance conditions. The transient absorption and coherent phonon amplitudes were measured as a function of the angle between the pump and probe polarizations and were analyzed based on the absorption anisotropy of carbon nanotubes. © *2009 American Institute of Physics*.
[DOI: 10.1063/1.3126715]

I. INTRODUCTION

In recent years, single-walled carbon nanotubes (SWNTs) have been intensively studied in various fields because of their unique optical and electrical characteristics. Wildoer *et al.*[1] directly observed electronic density of states of individual SWNTs by scanning tunneling spectroscopy, and Rao *et al.*[2] showed resonance Raman spectra of SWNTs for a wide energy region. SWNTs can be described as a graphene sheet rolled into a cylindrical shape having a large aspect ratio between its diameter and its length such that it can be considered as quasi-one-dimensional nanostructure with axial symmetry. Because of the large structural anisotropy, the optical properties of SWNT strongly depend on the incident light polarization, and the absorption is diminished for polarizations perpendicular to the nanotube axis.[3–7]

For a carbon nanotube, the chirality is given as a single vector that corresponds to a section of the nanotube perpendicular to the nanotube axis, and by which the types of SWNTs are classified. The vector can be expressed by two integers (n,m) that define the circumferential length and the chiral angle of the nanotubes. Except for very small diameter nanotubes, it is well known that structures for which n-m is evenly divisible by three display metallic or semimetallic behavior, whereas other tubes just slightly different in structure can have significant band gap showing semiconducting behavior.[8] The quasi-one-dimensionality of SWNTs gives sharp van Hove peaks in the electronic density of states. Optical properties of SWNTs are dominated by excitonic resonances associated with transitions between corresponding van Hove peaks of the valence and the conduction bands. Energies of these E_{ii} van Hove transitions for specific (n,m) structures are important not only for absorption spectroscopy but also for resonant Raman spectroscopy.[2,9,10] A number of peaks in absorption and photoluminescence (PL) spectra reveal different types of tubes. For the anisotropic optical absorption properties of SWNTs, the intensities of these absorption bands gradually decrease with increasing polarization angle of the incident light relative to the tube axis.[11] Also, coherent phonon oscillation and resonant Raman spectroscopy provide resonant frequencies of the nanotubes, and the chiralities can be assigned from diameters relative to the frequency and resonant excitation energies.[12] In this paper, we report on the polarization dependence of a transient carrier dynamics and coherent phonon generation in individualized SWNTs using femtosecond pulses.

II. EXPERIMENT

Using a Ti:sapphire laser, we have performed degenerate pump-probe spectroscopy to investigate transient carrier dynamics and coherent phonon generation. Such a technique enables real-time observation of carrier and phonon dynamics for a wide excitation energy range accessible from a Ti:sapphire oscillator.[12] Coherent phonons can be excited by a femtosecond pulse, which is shorter than a phonon period. The generated coherent lattice oscillations are observed as modulations in the time-resolved transmission measurements. For polarization-resolved measurements on a SWNT sample, a $\lambda/2$ plate was used on a pump beam path and was rotated by using a stepping motor with a 15° step, while the probe beam polarization was fixed in the horizontal direction. With a tuning range between 730 and 850 nm of the Ti:sapphire oscillator having a pulse duration of 35 fs, the center wavelengths become relevant to resonant and off-resonant energies of a specific-chirality SWNT.[13,14] A noncollinear geometry was used with a pump beam spot size of ~60 μm in the overlap area. The studied sample is a

a)Electronic mail: kyee@cnu.ac.kr.

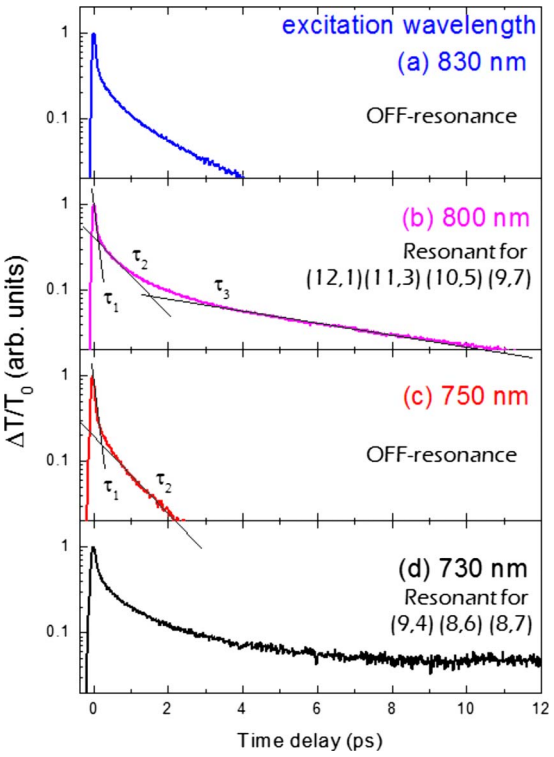

FIG. 1. (Color online) Transient pump-probe data as a function of time delay for different excitation wavelengths. [(a) and (c)] Off-resonance. (b) Resonant to (12,1) (11,3), (10,5), and (9,7) nanotubes. (d) Resonant to (9,4), (8,6), and (8,7) nanotubes. The resonant chiralities were taken from the PLE data. The pump-probe signal was fitted by three-exponential decaying functions for the resonant excitation cases and two-exponential decaying functions for the off-resonant conditions.

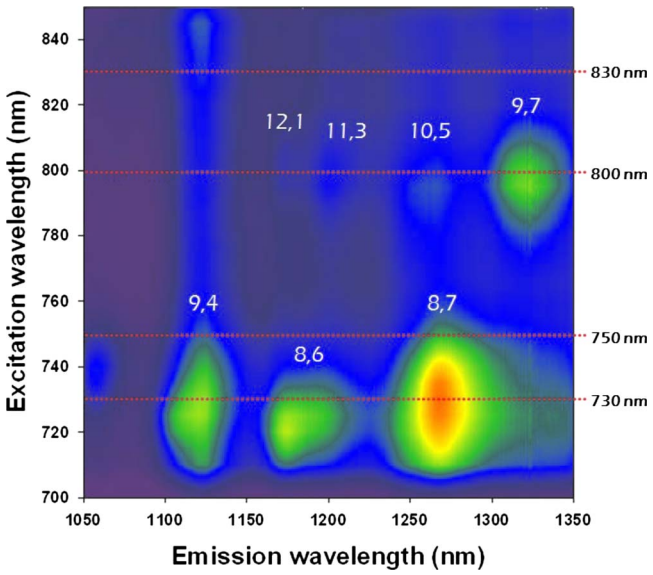

FIG. 2. (Color online) PLE spectra of SWNTs excited from 700 to 950 nm and detected from 950 to 1650 nm. (9,4), (8,6), and (8,7) are resonantly excited at the 730 nm and (11,3), (10,5), and (9,7) from the 800 nm excitation. 750 and 830 nm correspond to off-resonant excitations.

micelle-suspended SWNT solution, which is suspended individually with sodium cholate.[15] SWNTs exist in random directions in solution since they are flexible for rotational motions. PL excitation (PLE) spectroscopy was performed, and the PL was measured by changing the excitation wavelength from 700 to 950 nm using a cw-Ti:sapphire laser.

III. RESULTS AND DISCUSSION

Figures 1(a)–1(d) show transient transmission change as a function of time delay between pump and probe pulses, where four traces were obtained at different wavelengths of 730, 750, 800, and 830 nm, respectively. As can be checked with the PLE spectrum in Fig. 2, the wavelength of 730 nm (1.698 eV) in Fig. 1(d) corresponds to the E_2H_2 resonant transition energy of the (9,4), (8,6), and (8,7) chirality nanotubes, and the 800 nm in Fig. 1(b) is resonant with the (12,1), (11,3), (10,5), and (9,7) nanotubes. On the other hand, off-resonant excitation wavelengths of 750 and 830 nm were chosen for comparison.[16] Both resonant and off-resonant excitations show a positive change in transmission, which is consistent with the band filling effect. Two fast exponential decay components τ_1 and τ_2 are shown at all excitation wavelengths, irrespective of resonant or off-resonant cases. The τ_1 values ranged between 50 and 76 fs with wavelength, and the τ_2 values are in the range from 540 to 670 fs, where the variations with wavelength can occur possibly due to the differences in the extra energy above the band edges for nonresonantly excited carbon nanotubes. The slow component with $\tau_3 \sim 3$ ps can be additionally found for resonant cases. When the pump pulse resonantly excites the nanotubes with the E_{22} energy, the following probe pulse with the same energy will have a less absorption, and the transient transmission will be increased. The carriers excited in the E_2 or H_2 energy state will relax down to the E_1 or H_1 energy states, with the transient transmission disappearing relatively slowly (τ_3) due to the interband transitions, $E_2 \rightarrow E_1$ or $H_2 \rightarrow H_1$. On the other hand, if the first pulse off-resonantly excites the nanotubes with energy larger than the E_{22} energy, carriers will fill the states with additional energy. As such, the thermal distribution is described by a Maxwell–Boltzmann distribution of photoexcited carriers,[17] which is established by rapid carrier-carrier scattering with τ_1, and the relaxation process to the E_{22} energy minimum state will be followed with a characteristic time of τ_2.

To understand the optical anisotropic properties of SWNTs, we performed polarization-dependent pump-probe measurements. The excitation polarization of the pump was varied from parallel to perpendicular orientations relative to probe polarization. The pump-probe signal was fitted by three-exponentially decay functions of $\Delta T/T_0 = A_1 \exp(-t/\tau_1) + A_2 \exp(-t/\tau_2) + A_3 \exp(-t/\tau_3)$ for the resonant excitation cases. Figure 3 shows amplitudes of (A_1, A_2, and A_3) for each decay contributions as a function of the polarization angle of the pump beam at the resonant excitation of 800 nm. The pump-probe signal amplitudes reach maxima around 0°, while having minimum values when pump polarization is perpendicular to the probe polarization. The equation $y = A(1 + 2\cos^2\theta) + B$ is a good fit to the experimental results, with θ being the angle between the pump and probe polarizations. The polarization-dependent behavior is related to the absorption anisotropy of carbon nanotubes, where detailed analysis will be described in the later part of this manuscript.

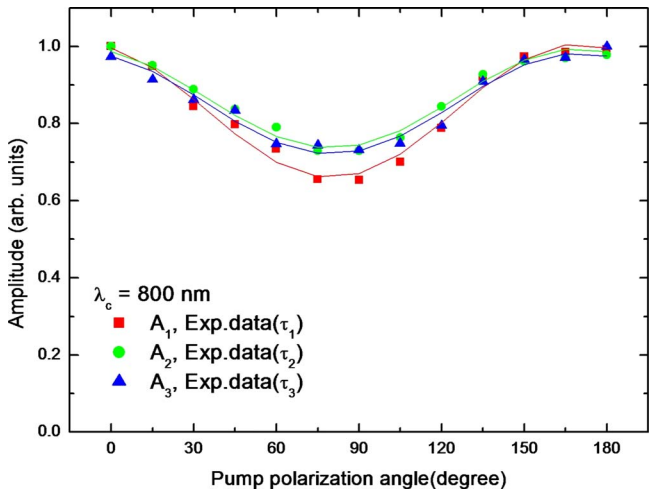

FIG. 3. (Color online) Amplitudes (A_1, A_2, and A_3) for each decay contribution of the transient transmission signal as a function of the pump polarization angle (θ) at the resonant excitation of 800 nm.

We observed that the pump-probe signal contains phonon-induced oscillations. Figure 4(a) shows the coherent phonon oscillations at an excitation wavelength of 800 nm at different pump polarizations. There are beatings on the signal because a number of nanotubes with different frequencies are oscillating simultaneously. Figure 4(b) shows a Fourier-transformed (FT) spectrum in the frequency domain obtained from the coherent phonon oscillations. Each peak reflects the radial breathing mode of a specific-chirality carbon nanotube. The FT spectrum is fitted to a Lorentzian function to obtain the peak frequency, intensity, and FWHM. Based on these fitting parameters, chirality indices (n,m) were assigned.

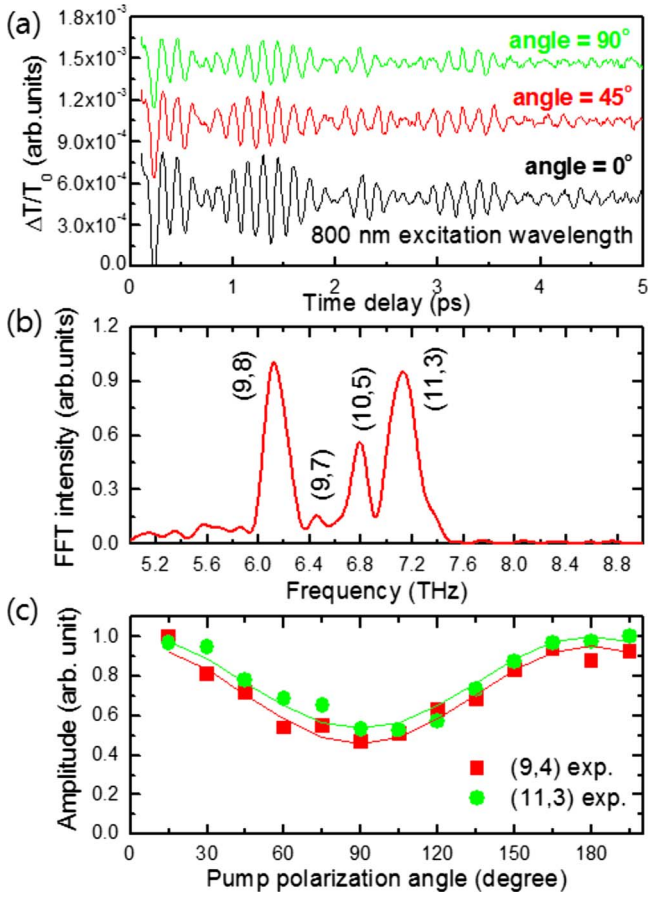

FIG. 4. (Color online) (a) Coherent phonon oscillation at 800 nm for different pump polarization. (b) FT power spectrum at 800 nm for pump polarization of 0°. (c) Amplitude of coherent phonon oscillations of specific chiralities, (9,4) and (11,3) as a function of the pump polarization angle.

Figure 4(c) shows the polarization dependence of the RBM intensity for both (9,4) nanotubes resonant at 770 nm and (11,3) nanotubes resonantly excited at 800 nm, respectively. It is interesting that the coherent phonon oscillation has 180° periodicity with respect to θ, the same as the polarization-dependent carrier dynamics shown in Fig. 3. As compared with the parallel angle (0°) of the incident beam for both cases, the coherent phonon amplitude is weakened at the perpendicular angle (90°) of the pump beam. Although the amplitude is decreased at 90°, it does not disappear completely, and the phonon intensity can also be fitted well with the $y=A(1+2\cos^2\theta)+B$ function. This can be explained in the following manner. The nanotubes in the solution sample exist with random directions within the pump beam spot. Although the incident light polarization is precisely perpendicular to a certain nanotube, other tubes parallel with the light polarization in the sample can be excited and will contribute to the pump-probe signal.[18] To help us with this understanding, we have calculated the polarization-dependent coherent phonon generation by a simple model in Fig. 5. The polarization of the pump is varied with respect to the probe with an angle θ, and the polarization of the nanotubes is changed with angle φ. When the incident pump beam, probe beam, and nanotubes have the same direction of polarization, the intensity equals unity. As the pump polarization is varied with respect to the nanotubes with an angle $\varphi-\theta$, the coherent phonon intensity generated by the pump beam will be reduced to $1\cos^2(\varphi-\theta)$. The measured intensity reduction due to the probe polarization will be proportional to $\cos^2(\varphi)$. The total coherent phonon intensity relative to the random angle of the nanotubes can be expressed as

$$I(\theta) \propto \int_0^{2\pi} \cos^2(\varphi-\theta)\cos^2\varphi d\varphi = 2\cos^2\theta + 1. \qquad (1)$$

The graph in Fig. 5 shows both the calculation and the experimental results. The curve represents theoretical calculations and the squares are experimental values. The maximum intensity of the experimental results is 1.86 times higher than the minimum, with the fitting parameters of A and B, being 0.234 and 0.302, respectively. We note that the fitting parameter B was used considering an angle-independent contribution.

IV. CONCLUSIONS

In conclusion, we have demonstrated anisotropic features of transient carrier dynamics and coherent phonon generation in SWNTs. We observed carrier dynamics containing two-decay components under off-resonant excitation and found an additional longer decay component in resonant cases. From PLE and coherent phonon data, we suggest that the two shorter decay components originated from metallic

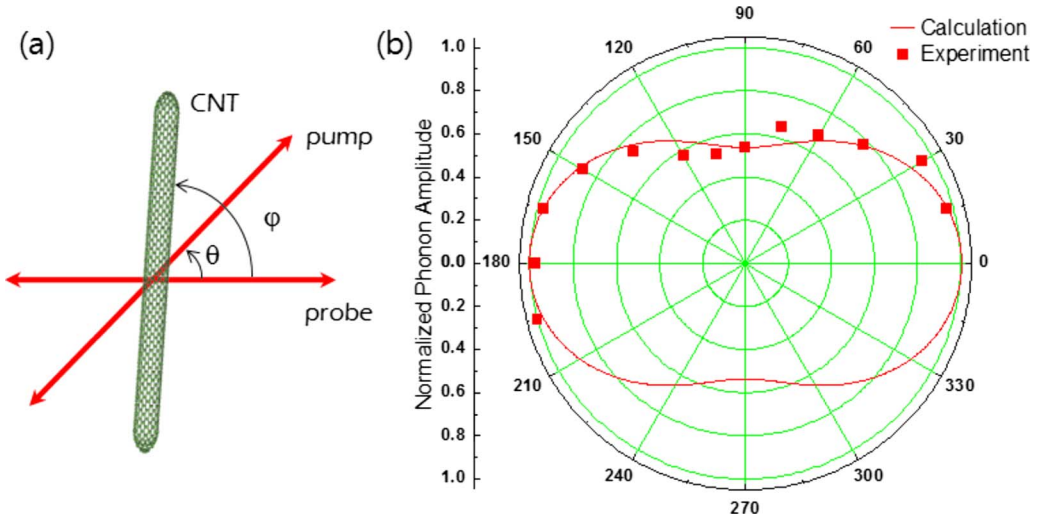

FIG. 5. (Color online) Schematic for the polarization-dependent coherent phonon oscillation and polar plot for normalized phonon amplitude as a function of the relative pump polarization angle (θ).

nanotubes, while the additional longer decay is derived from semiconducting nanotubes. We presented a simple model to successfully explain the observed polarization-dependent carrier dynamics and coherent phonon oscillations, correctly taking into account the optical anisotropy of the nanotubes.

ACKNOWLEDGMENTS

This work was supported by the Korea Research Foundation Grant funded by the Korean Government (MOEHRD, Basic Research Promotion Fund) (Grant No. KRF-2007-313-C00308), the Korea Science and Engineering Foundation (Grant Nos. 2008-03535, R11-2008-095-01000-0, R01-2007-000-20651-0), the National Science Foundation (Grant Nos. OISE-0530220 and DMR-0325474), and the Robert A. Welch Foundation (Grant No. C-1509).

[1]J. W. G. Wilder, L. C. Venema, A. G. Rinzler, R. E. Smalley, and C. Dekker, Nature (London) **391**, 59 (1998).
[2]A. M. Rao, E. Richter, S. Bandow, B. Chase, P. C. Eklund, K. A. Williams, S. Fang, K. R. Subbaswamy, M. Menon, A. Thess, R. E. Smallys, G. Dresselhaus, and M. S. Dresselhaus, Science **275**, 187 (1997).
[3]G. S. Duesberg, I. Loa, M. Burghard, K. Syassen, and S. Roth, Phys. Rev. Lett. **85**, 5436 (2000).
[4]J. Lefebvre, J. M. Fraser, P. Finnie, and Y. Homma, Phys. Rev. B **69**, 075403 (2004).
[5]J. Guo, C. Yang, Z. M. Li, M. Bai, H. J. Liu, G. D. Li, E. G. Wang, C. T. Cham, Z. K. Tang, W. K. Ge, and X. Xiao, Phys. Rev. Lett. **93**, 017402 (2004).
[6]Y. Hashimoto, Y. Murakami, S. Maruyama, and J. Kono, Phys. Rev. B **75**, 245408 (2007).
[7]J. Lefebvre and P. Finnie, Phys. Rev. Lett. **98**, 167406 (2007).
[8]N. Hamada, S. Sawada, and A. Oshiyama, Phys. Rev. Lett. **68**, 1579 (1992).
[9]M. S. Dresselhaus, G. Dresselhaus, A. Jorio, A. G. Souza Filgo, M. A. Pimenta, and G. Saito, Acc. Chem. Res. **35**, 1070 (2002).
[10]H. Kuzmany, W. Plank, M. Hulman, Ch. Kramberger, A. Gruneis, Th. Pichler, H. Peterlik, H. Kataura, and Y. Achiba, Eur. Phys. J. B **22**, 307 (2001).
[11]Z. M. Li, Z. K. Tang, H. J. Liu, N. Wang, C. T. Chan, R. Saito, S. Okada, G. D. Li, J. S. Chen, N. Nagasawa, and S. Tsuda, Phys. Rev. Lett. **87**, 127401 (2001).
[12]Y.-S. Lim, K.-J. Yee, J.-H. Kim, E. H. Hároz, J. Shaver, J. Kono, S. K. Doorn, R. H. Hauge, and R. E. Smalley, Nano Lett. **6**, 2696 (2006).
[13]G. C. Cho, W. Kutt, and H. Kurz, Phys. Rev. Lett. **65**, 764 (1990).
[14]R. B. Weisman and S. M. Bachilo, Nano Lett. **3**, 1235 (2003).
[15]M. J. O'Connell, S. M. Bachilo, C. B. Huffman, V. C. Moore, M. S. Strano, E. H. Hároz, K. L. Rialon, P. J. Boul, W. H. Noon, C. Kittrell, J. Ma, R. H. Hauge, R. B. Weisman, and R. E. Smalley, Science **297**, 593 (2002).
[16]G. N. Ostojic, S. Zaric, J. Kono, M. S. Strano, V. C. Moore, R. H. Hauge, and R. E. Smalley, Phys. Rev. Lett. **92**, 117402 (2004).
[17]T. Hertel, R. Fasel, and G. Moos, Appl. Phys. A: Mater. Sci. Process. **75**, 449 (2002).
[18]K. Kato, K. Ishioka, M. Kitajima, J. Tang, R. Saito, and H. Petek, Nano Lett. **8**, 3102 (2008).